Supporting Information

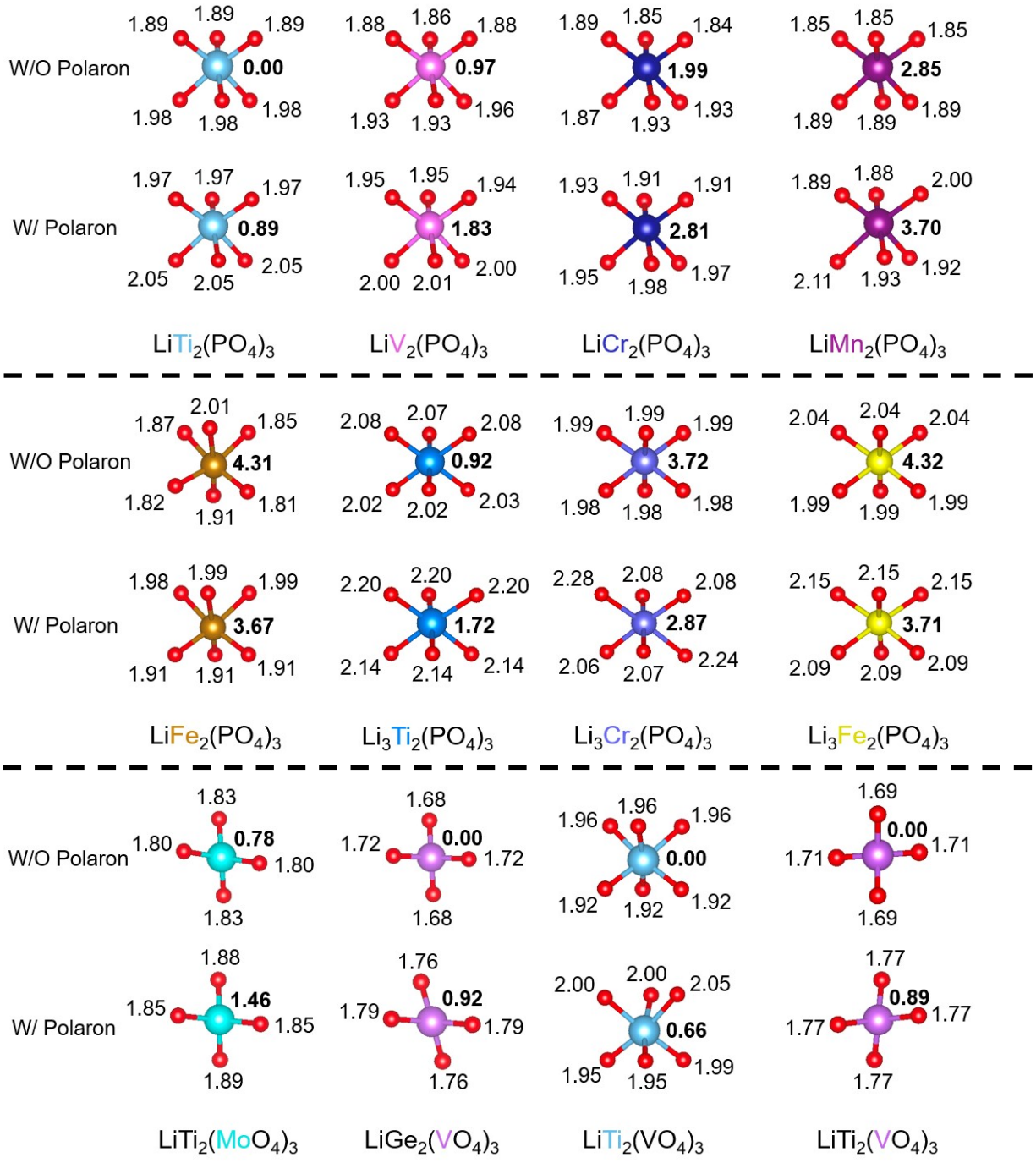

Figure S1. The TM-O bond lengths (Å) of pristine and polaronic local structures in Li-NASICONs. Bold letters denote magnetic moments of the TM atoms. Different colored spheres denote TM atoms, red spheres denote O atoms. The numbers near oxygen atoms denote TM-O bond lengths in Å, bold numbers near the center TM atoms denote their magnetic moments.

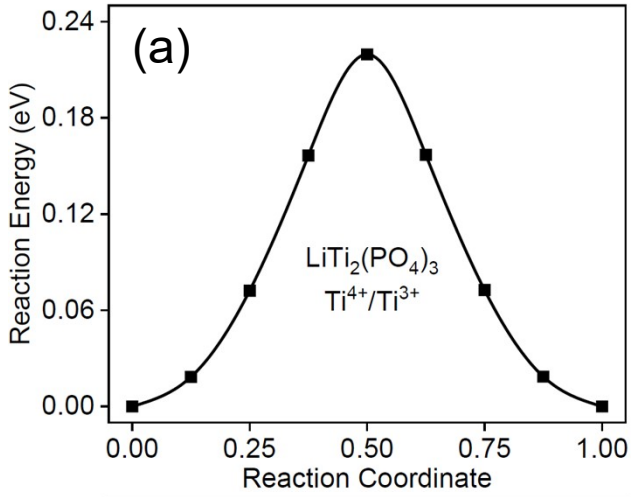
(a)
Reaction Energy (eV)
Reaction Coordinate
$LiTi_2(PO_4)_3$
Ti^{4+}/Ti^{3+}

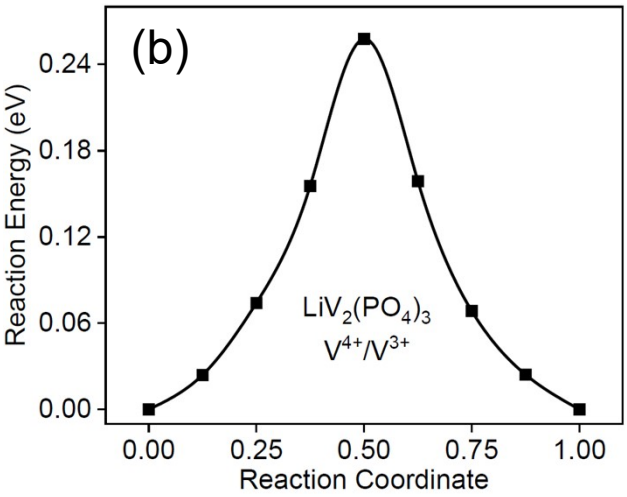
(b)
Reaction Energy (eV)
Reaction Coordinate
$LiV_2(PO_4)_3$
V^{4+}/V^{3+}

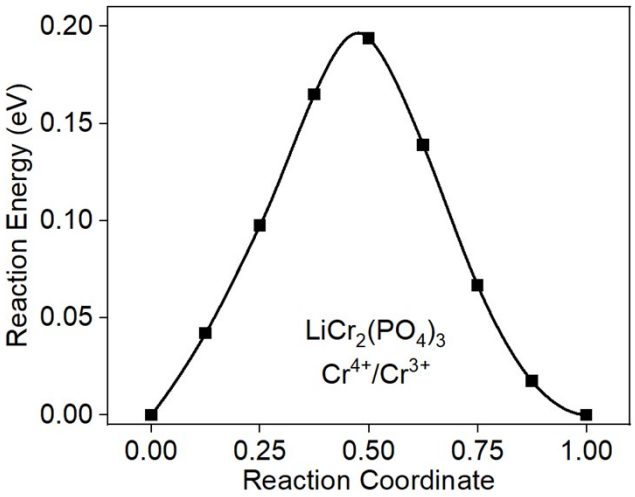
Reaction Energy (eV)
Reaction Coordinate
$LiCr_2(PO_4)_3$
Cr^{4+}/Cr^{3+}

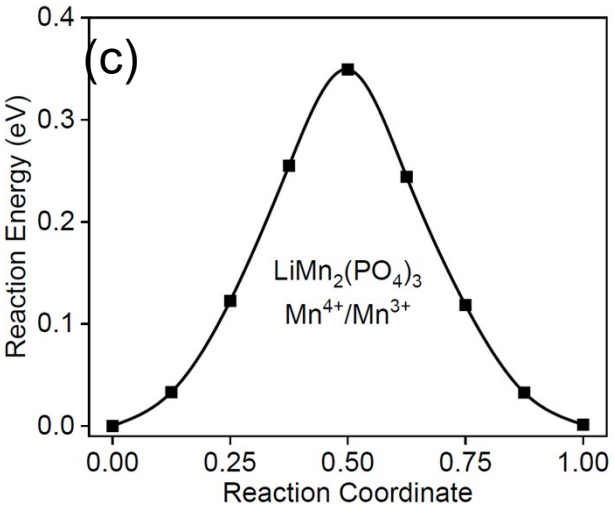
(c)
Reaction Energy (eV)
Reaction Coordinate
$LiMn_2(PO_4)_3$
Mn^{4+}/Mn^{3+}

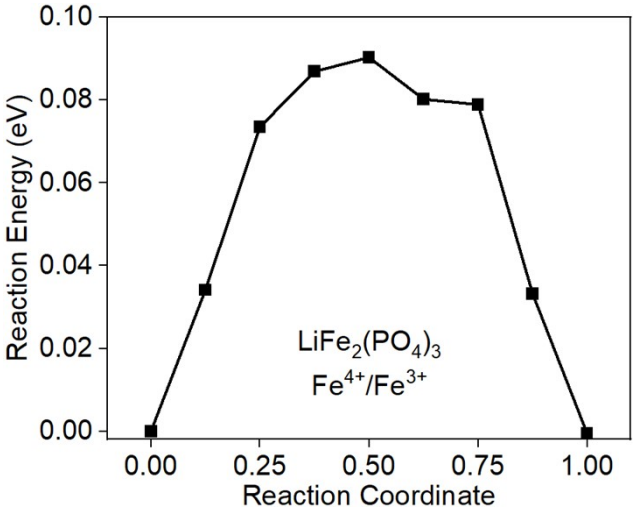
Reaction Energy (eV)
Reaction Coordinate
$LiFe_2(PO_4)_3$
Fe^{4+}/Fe^{3+}

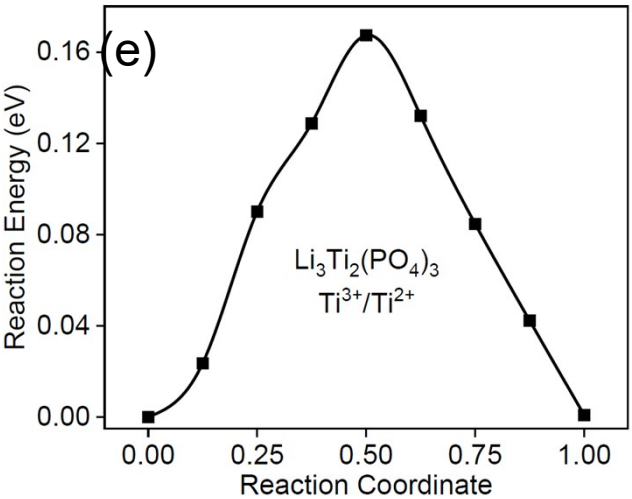
(e)
Reaction Energy (eV)
Reaction Coordinate
$Li_3Ti_2(PO_4)_3$
Ti^{3+}/Ti^{2+}

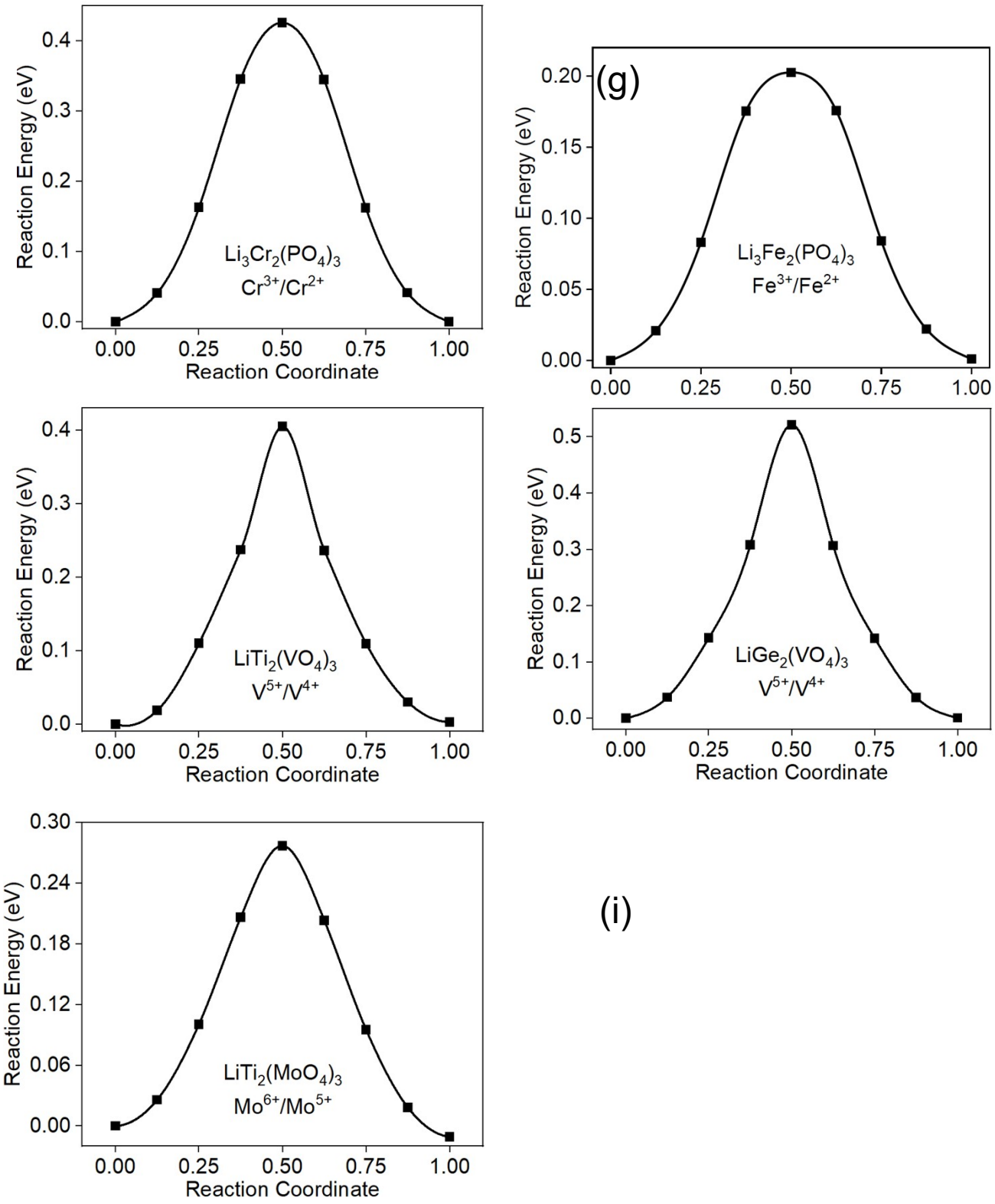

Figure S2. Polaron hopping energy curves of (a) $LiTi_2(PO_4)_3$ (b) $LiV_2(PO_4)_3$ (c) $LiCr_2(PO_4)_3$ (d) $LiMn_2(PO_4)_3$ (e) $LiFe_2(PO_4)_3$ (f) $Li_3Ti_2(PO_4)_3$ (g) $Li_3Cr_2(PO_4)_3$ (h) $Li_3Fe_2(PO_4)_3$ (i) $LiTi_2(VO_4)_3$ (j) $LiGe_2(VO_4)_3$ (k) $LiTi_2(MoO_4)_3$.

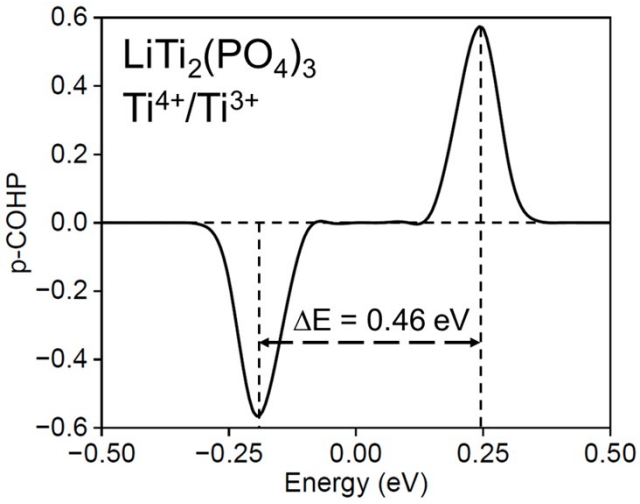
LiTi2(PO4)3
Ti4+/Ti3+
ΔE = 0.46 eV
p-COHP
Energy (eV)

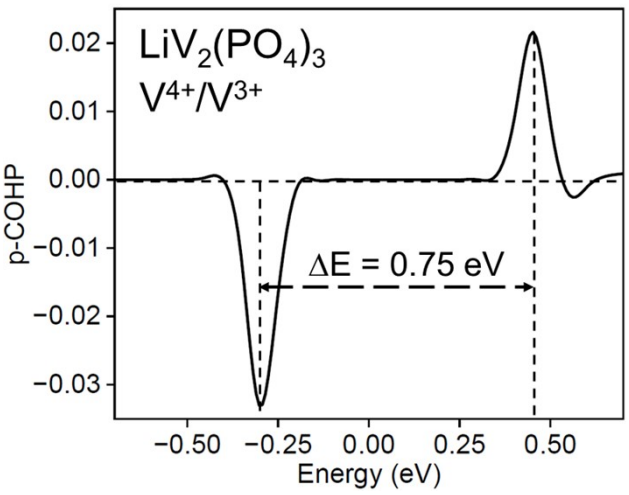
LiV2(PO4)3
V4+/V3+
ΔE = 0.75 eV
p-COHP
Energy (eV)

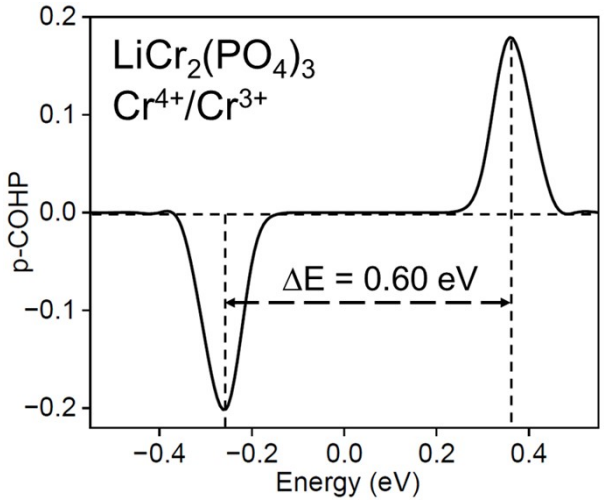
LiCr2(PO4)3
Cr4+/Cr3+
ΔE = 0.60 eV
p-COHP
Energy (eV)

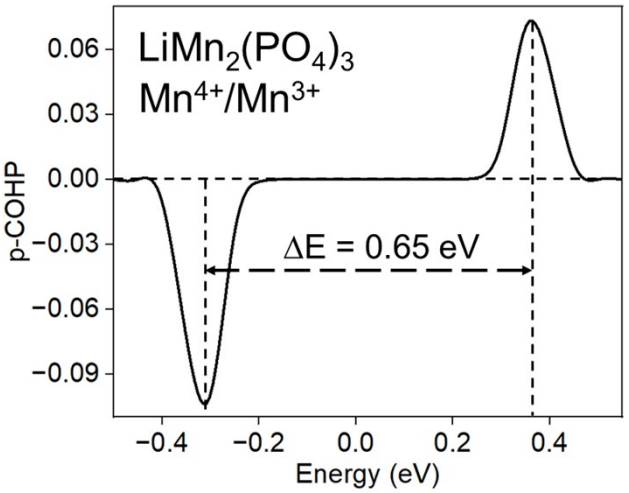
LiMn2(PO4)3
Mn4+/Mn3+
ΔE = 0.65 eV
p-COHP
Energy (eV)

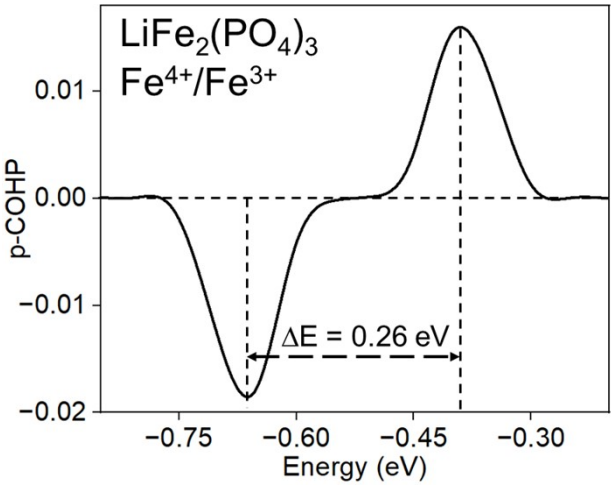
LiFe2(PO4)3
Fe4+/Fe3+
ΔE = 0.26 eV
p-COHP
Energy (eV)

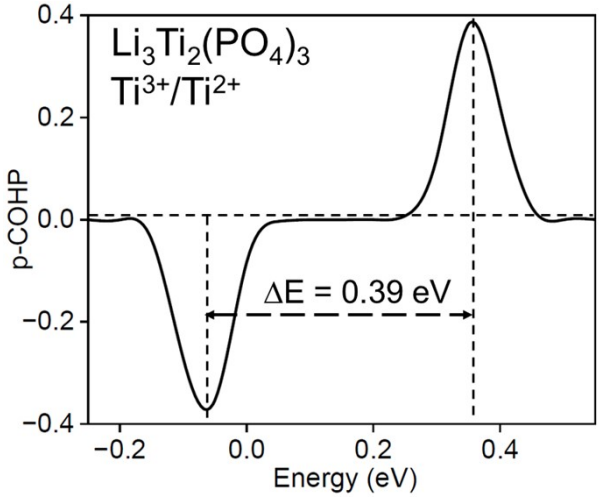
Li3Ti2(PO4)3
Ti3+/Ti2+
ΔE = 0.39 eV
p-COHP
Energy (eV)

(a) (b)

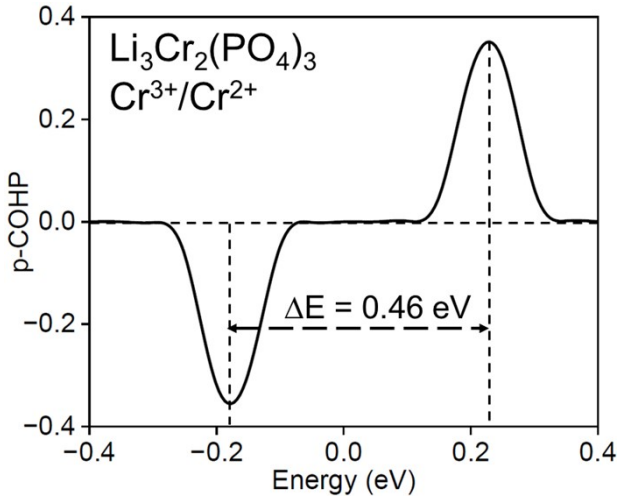
$Li_3Cr_2(PO_4)_3$
Cr^{3+}/Cr^{2+}
ΔE = 0.46 eV
p-COHP
Energy (eV)

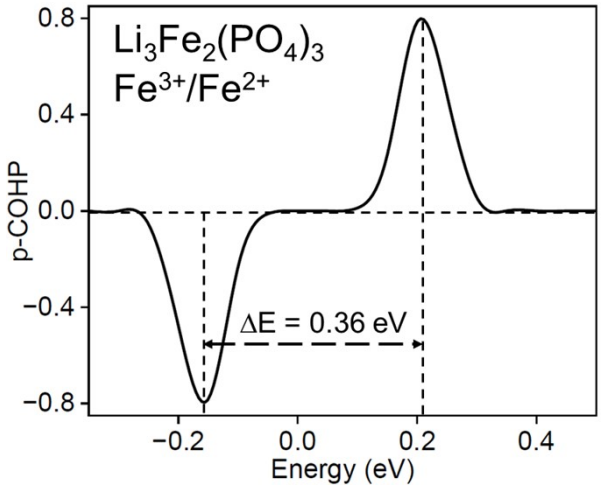
$Li_3Fe_2(PO_4)_3$
Fe^{3+}/Fe^{2+}
ΔE = 0.36 eV
p-COHP
Energy (eV)

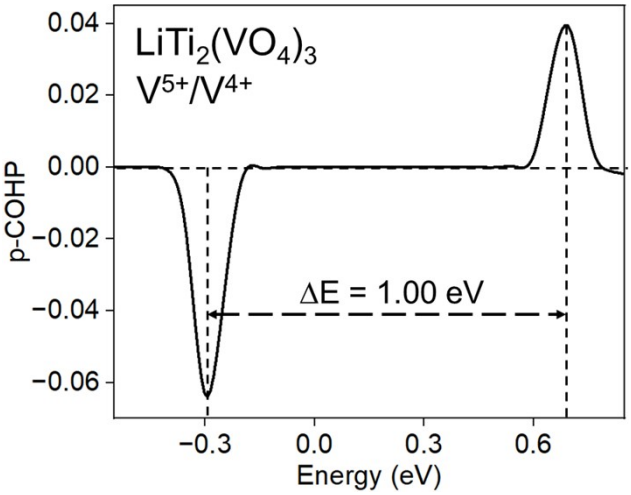
$LiTi_2(VO_4)_3$
V^{5+}/V^{4+}
ΔE = 1.00 eV
p-COHP
Energy (eV)

(g)

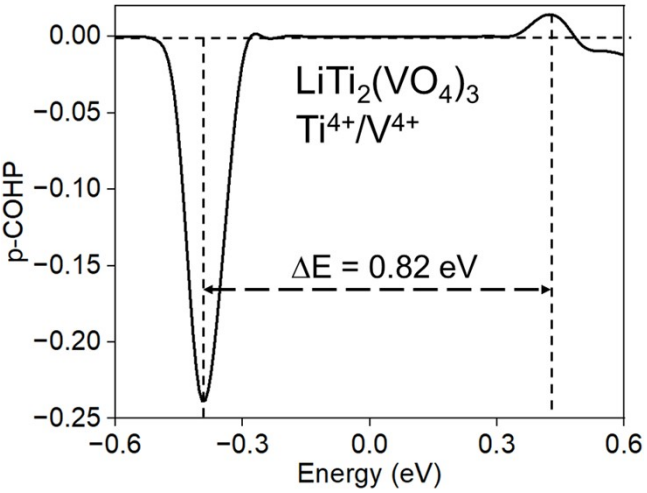
$LiTi_2(VO_4)_3$
Ti^{4+}/V^{4+}
ΔE = 0.82 eV
p-COHP
Energy (eV)

(h)

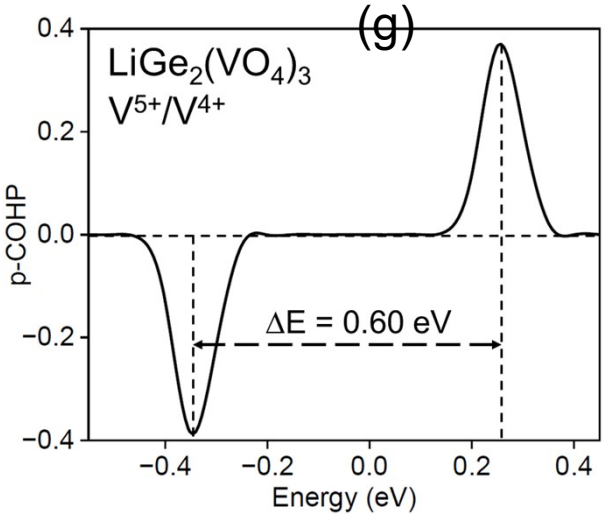
$LiGe_2(VO_4)_3$
V^{5+}/V^{4+}
ΔE = 0.60 eV
p-COHP
Energy (eV)

(i)

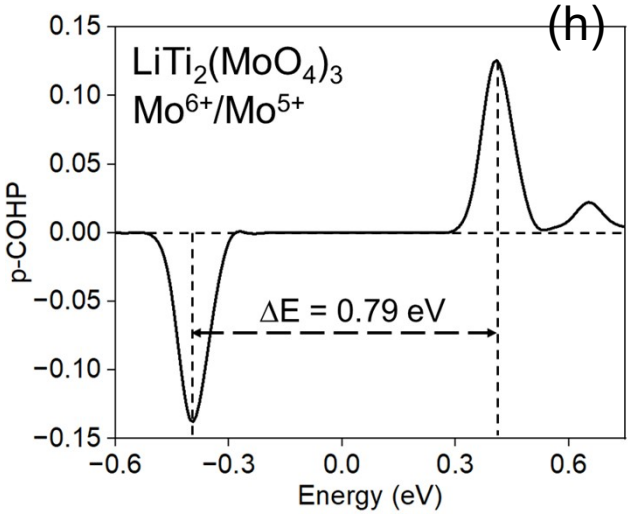
$LiTi_2(MoO_4)_3$
Mo^{6+}/Mo^{5+}
ΔE = 0.79 eV
p-COHP
Energy (eV)

(j)

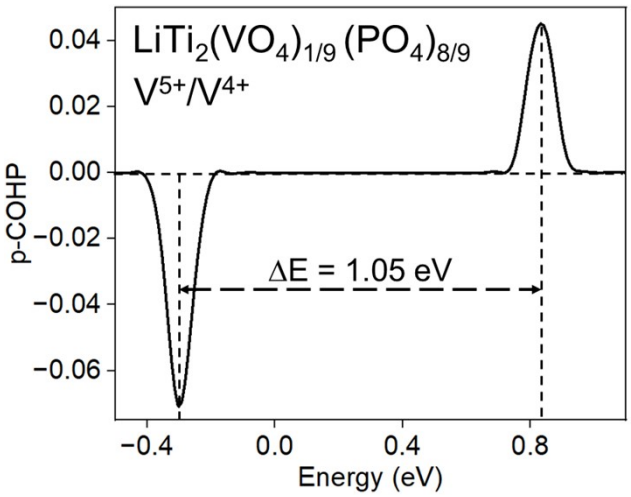

(m)

Figure S3. Polaronic bonding states and antibonding states of (a) $LiTi_2(PO_4)_3$. (b) $LiV_2(PO_4)_3$. (c) $LiCr_2(PO_4)_3$. (d) $LiMn_2(PO_4)_3$. (e) $LiFe_2(PO_4)_3$. (f) $Li_3Ti_2(PO_4)_3$. (g) $Li_3Cr_2(PO_4)_3$. (h) $Li_3Fe_2(PO_4)_3$. (i) $LiTi_2(VO_4)_3$ with tet-tet hopping. (j) $LiTi_2(VO_4)_3$ with oct-tet hopping. (k) $LiGe_2(VO_4)_3$ (l) $LiTi_2(MoO_4)_3$. (m) $LiTi_2(VO_4)_{1/9}(PO_4)_{8/9}$. ΔE denotes the energy gap between polaronic bonding and antibonding states. The charge transfer integral is estimated to be ½ ΔE.

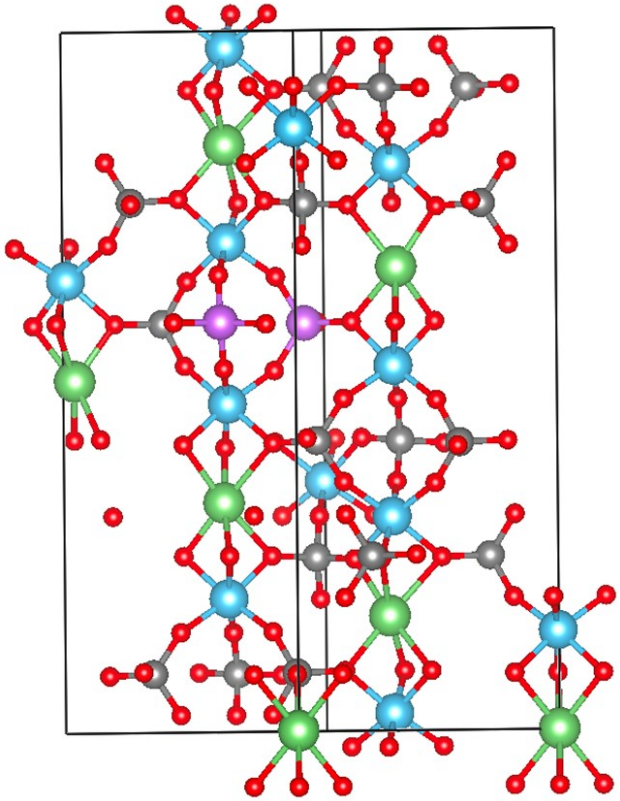

Figure S4. Crystal models for the simulation of polaron hopping in $LiTi_2(VO_4)_{1/9}(PO_4)_{8/9}$. Green spheres denote Li, blue spheres denote Ti, gray spheres denote P, purple spheres denote V and red spheres denote O.

Table S1. Bond lengths of Jahn-Teller distortion active TM-O_6 octahedron in Li-NASICONs.

	Bond 1	Bond 2	Bond 3	Bond 4	Bond 5	Bond 6
Fe^{4+}-O_6	1.87	2.01	1.85	1.82	1.91	1.81
Mn^{3+}-O_6	1.89	1.88	2.00	2.11	1.90	1.92
Cr^{2+}-O_6	2.28	2.08	2.08	2.06	2.07	2.24

Unit: Å

Table S2. The lattice volumes of Li-NASICONs.

$LiTi_2(PO_4)_3$	1311.31
$LiV_2(PO_4)_3$	1271.79
$LiCr_2(PO_4)_3$	1239.68
$LiMn_2(PO_4)_3$	1215.19
$LiFe_2(PO_4)_3$	1186.21
$Li_3Ti_2(PO_4)_3$	1394.42
$Li_3Cr_2(PO_4)_3$	1315.96
$Li_3Fe_2(PO_4)_3$	1350.52
$LiTi_2(VO_4)_3$	1503.70
$LiGe_2(VO_4)_3$	1429.82
$LiTi_2(MoO_4)_3$	1666.99

Unit: $Å^3$

The electrochemical stability window is calculated by constructing the grand potential Ψ, which is a Legendre transformation of the enthalpy with respect to the lithium chemical potential, i.e., $\Psi = E - u_{Li} \times n_{Li}$, where E is the enthalpy of a Li-NASICON compound, u_{Li} is the lithium chemical potential, and n_{Li} is the Li concentration in each compound. To maintain compatibility with the Materials Project database, we compute the energies of each Li-NASICONs using the GGA/GGA+U functional. To construct the grand potential phase diagrams, we query all phases within each compound's respective chemical space from the Materials Project database. We determine the oxidative and reductive potential by scanning u_{Li} in increment of 0.01 eV to identify the chemical potential range where the Li-NASICON compound remains stable. We note that these electrochemical stability windows do not account for the possibility of Li (de)intercalation, which may occur due to potential mixed ionic electronic conductivities.

Table S3. The electromical stability window of Li-NASICONs considered in this work.

$LiTi_2(PO_4)_3$	2.15~4.64
$LiV_2(PO_4)_3$	3.53~4.01
$LiCr_2(PO_4)_3$	4.25~4.30
$LiMn_2(PO_4)_3$	4.28~4.34
$LiFe_2(PO_4)_3$	4.23~4.41
$Li_3Ti_2(PO_4)_3$	2.09~2.12
$Li_3Cr_2(PO_4)_3$	2.34~4.27
$Li_3Fe_2(PO_4)_3$	3.32~4.18
$LiTi_2(VO_4)_3$	3.19~3.91
$LiGe_2(VO_4)_3$	3.57~4.10

Unit: V (vs Li/Li^+)